Journal of the Geological Society, London, Vol. **157,** 2000, pp. 565–576. Printed in Great Britain.

Variscan collisional magmatism and deformation in NW Iberia: constraints from U–Pb geochronology of granitoids

J. FERNÁNDEZ-SUÁREZ[1,2], G. R. DUNNING[1], G. A. JENNER[1] & G. GUTIÉRREZ-ALONSO[3]

[1]*Department of Earth Sciences, Memorial University of Newfoundland, St John's, NF, Canada A1B 3X5*

[2]*Present address: Departamento de Petrología y Geoquímica, Facultad de Geología, Universidad Complutense, 28040 Madrid, Spain (e-mail: jfsuarez@eucmos.sim.ucm.es)*

[3]*Departamento de Geología, Facultad de Ciencias, Universidad de Salamanca, 37008 Salamanca, Spain (e-mail: gabi@usal.es)*

Abstract: U–Pb geochronology of Variscan granitoid rocks from the West Asturian Leonese Zone of the NW Iberian belt documents the episodic nature of magmatism in this section of the western European Variscides. Each magmatic episode is characterized by granitoids with distinct features and has a duration on the scale of several millions of years. The ages of these granitoids place new constraints on the age and duration of magmatic and tectonic events, that are consistent with previous structural studies and proposed models for the tectonic evolution and migration of deformation in the NW Iberian Variscan belt.

Granitoid rocks in this zone belong to two main magmatic episodes (syn- and post-tectonic relative to the Variscan Orogeny) and are broadly representative of the granitoid types found in the NW Iberian Variscan belt. The syntectonic association is formed by: (i) tonalite–granodiorite–monzogranite intrusions emplaced synchronously with the main phase of crustal deformation (D_2) at *c*. 325 Ma and (ii) younger leucogranite intrusions emplaced synchronously with syn-convergence extensional structures at *c*. 320–310 Ma. The post-tectonic association is composed of: (i) volumetrically dominant tonalite–granodiorite–monzogranite intrusions (and associated minor mafic-intermediate rocks) emplaced at *c*. 295–290 Ma; and (ii) scarce leucogranite intrusions emplaced at *c*. 290–285 Ma.

Keywords: Iberia, Variscides, granitoids, U/Pb, deformation.

The Variscan belt of NW Iberia is characterized by abundant granitoid plutonism and is one of the most intensively studied and better understood sections of the western European Variscides from a tectonic perspective (Pérez Estaún *et al*. 1991; Martínez Catalán *et al*. 1996, 1997; Dallmeyer *et al*. 1997 and references therein). In Iberia there have been however few geochronological studies, particularly those utilizing high precision U–Pb dating, used to constrain the timing of granitoid genesis and deformation during the Variscan collisional orogenic event.

In this paper, we present nine new U–Pb zircon and monazite ages for a range of granitoid types from the West Asturian Leonese Zone of the NW Iberian Variscan belt. This particular area was chosen because the relationships between granitoids and tectonic events have been well established (Martínez Catalán 1985; Bastida *et al*. 1986; Bellido *et al*. 1987; Martínez Catalán *et al*. 1990; Aranguren & Tubía 1992). Furthermore, previous isotopic studies in this area had difficulty obtaining reliable and precise isochron ages for these granitoids, particularly for the syntectonic intrusions (e.g. Bellido *et al*. 1992; Galán *et al*. 1996). This has prevented the substantiation of the structural chronology of magmatic events within a precise absolute time framework. The plutons studied are broadly representative of the main granitoid types found elsewhere in the autochthon of the NW Iberian Variscan belt.

The primary aim of this paper is to discuss the age of the granitoids and the constraints these ages place on the length and timing of the magmatic and deformation events in the West Asturian Leonese Zone of the Iberian Variscan belt. We also provide concise petrological and geochemical information to help the reader compare these granitoids to others in the Variscan belt. At the end of the paper we compare our data with those available from the neighbouring areas to the east and west of the West Asturian Leonese Zone, that is the Cantabrian and Central Iberian zones, respectively. We also discuss potential implications of these data for models for the tectonic evolution of the Variscan collisional orogen in NW Iberia.

Geological background

The geology of the NW Iberian Variscan belt has been extensively studied and the main stratigraphic, structural, metamorphic and igneous features and geodynamic evolution are described in comprehensive contributions (e.g. Capdevila *et al*. 1973; Corretgé 1983; Martínez *et al*. 1988; Martínez Catalán *et al*., 1990; Pérez Estaún *et al*. 1990, 1991; Dallmeyer *et al*. 1997; Martínez Catalán *et al*. 1996, 1997). The area selected for this study is the West Asturian Leonese Zone of the Iberian Variscan belt (Fig. 1). This zone is the transition between the foreland areas (Cantabrian Zone, to the east) and the hinterland, represented by the Central Iberian zone to the west. These zones comprise the NW Iberian Variscan relative autochthon (see references above).

The West Asturian Leonese Zone consists of an Upper Proterozoic flyschoid series unconformably overlain by a thick, mostly siliciclastic Paleozoic pre-orogenic sequence. The main structural features of the West Asturian Leonese Zone are attributed to three major phases of Variscan deformation.

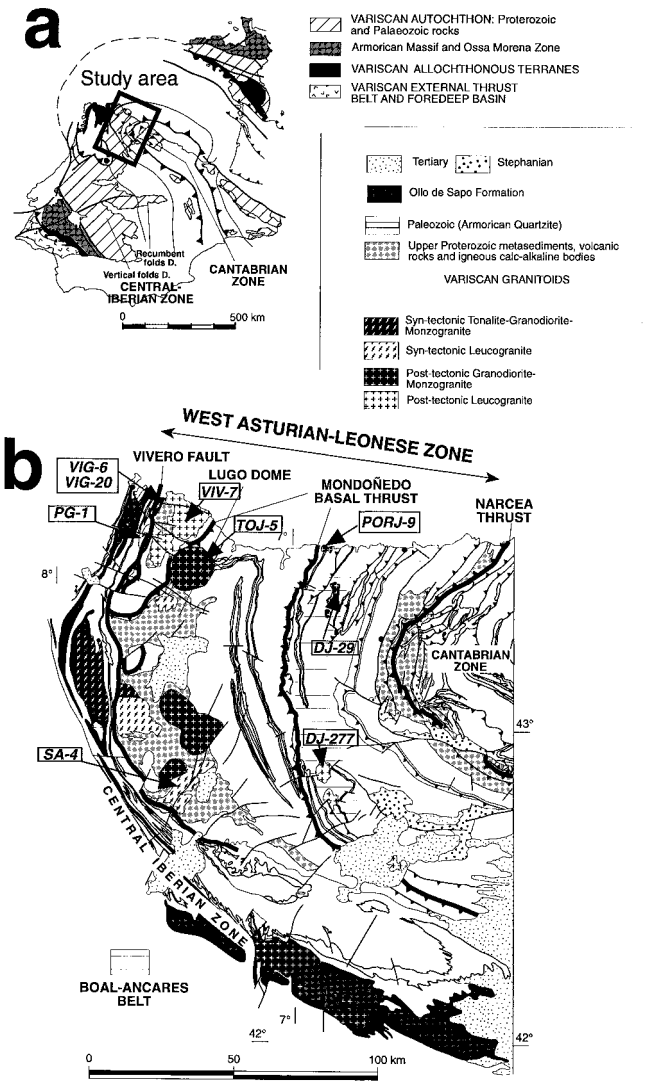

Fig. 1. (**a**) Sketch showing the main Variscan outcrops in Iberia, with the location of the study area. (**b**) Geological map of the West Asturian Leonese zone of the Iberian Variscan belt showing the main units, structures and granitoid rocks. References in italics indicate the location of samples dated by U–Pb.

The first phase (D_1) produced large recumbent folds with a vergence towards the external part of the orogenic belt. A primary cleavage (S_1) was developed in relation to these folds. The second deformation phase (D_2) produced thrust structures and associated shear zones. The most important of these structures in the study area are the basal fault and shear zone of the Mondoñedo thrust sheet to the west and the Narcea–Trones shear zones to the east (Fig. 1). Based on ^{40}Ar–^{39}Ar ages of syn-D_1 and syn-D_2 metamorphic fabrics (Dallmeyer *et al.* 1997) the main episode of crustal shortening in the study area took place between *c.* 330 and 315 Ma. The third deformation phase (D_3) produced large open folds approximately co-axial with the D_1 folds, together with minor folds and the local development of a crenulation cleavage (S_3).

The western limit of the West Asturian Leonese Zone is a north–south-striking fault (Vivero fault, Fig. 1) which has been interpreted as a ductile, normal, extensional shear zone developed in response to crustal thickening in a larger scale transpressive regime (Aranguren & Tubía 1992; Martínez *et al.* 1996; Reche *et al.* 1998). The Vivero fault truncates the shear zones associated with the Mondoñedo Nappe (D_2) (Martínez Catalán 1985; Aranguren & Tubía 1992). However, the structural data provided by Aranguren & Tubía (1992) indicate that extensional motion on the Vivero fault overlapped in time with thrusting of the Mondoñedo Nappe, and can therefore be considered a syn- to post-D_2 and pre-D_3 structure. Evidence for syn-convergence extension has been reported from other areas of the NW Iberian Variscan belt (e.g. Escuder Viruete *et al.* 1994; Díez Balda *et al.* 1995; Valverde-Vaquero *et al.* 1995; Martínez Catalán *et al.* 1996; Ayarza *et al.* 1998).

Regional metamorphism in the West Asturian Leonese Zone increases in grade from east to west and is characterized by the zonal Barrovian-type sequence chlorite–biotite–almandine–staurolite–(kyanite). This medium pressure metamorphic event (M_1) reached its climax during the D_1–D_2 interphase (Bastida *et al.* 1986; Suárez *et al.* 1990; Martínez Catalán *et al.* 1990). A later high temperature–low pressure metamorphic episode (M_2), characterized by the appearance of andalusite–sillimanite parageneses and the local development of migmatites, is recorded in the western part of the West Asturian Leonese Zone (Lugo Dome). The M_2 event occurred over a time span that extends from syn-D_2 to syn-D_3 and reached its climax during the D_2–D_3 interphase (Bastida *et al.* 1986). Finally, very low pressure parageneses with post-D_3 andalusite ± cordierite were developed as a consequence of the intrusion of post-tectonic granitoids both in the Lugo dome and in the eastern West Asturian Leonese Zone (Boal–Ancares belt, Fig. 1) (Fernández-Suárez 1994).

Plutonic rocks in the West Asturian Leonese Zone

Variscan granitoids are the main magmatic feature of the West Asturian Leonese Zone, although pre-Variscan igneous rocks are also present in this zone (e.g. Fernández-Suárez *et al.* 1998). Figure 1 illustrates that granitoids in this zone occur along two belts that follow the structural pattern of the orogenic belt in the area, the Lugo Dome to the west and the Boal–Ancares belt to the east.

On the basis of their structural relationships, Variscan granitoid rocks in the West Asturian Leonese Zone can be divided in two main associations: (i) syntectonic granitoids, and (ii) post-tectonic granitoids (Fig. 1) (see also Capdevila *et al.* 1973; Corretgé 1983; Corretgé *et al.* 1990; Bellido *et al.* 1987). The main petrological features of the granitoids allow these associations to be further subdivided into: (a) tonalite–granodiorite–monzogranite (TGM) intrusions; and (b) leucogranite intrusions. Both petrological groups are present in the syn- and post-tectonic granitoid associations. The main petrological and geochemical features of these groups are briefly described below and summarized in Fig. 2.

(ia) Syntectonic tonalite–granodiorite–monzogranite plutons

These plutons are the earliest Variscan granitoids in the West Asturian Leonese Zone, they cut across D_1 structures and were intruded synkinematically with the D_2 phase. They are formed by amphibole–biotite tonalites and quartz diorites, biotite ± amphibole granodiorites (common rock type) and biotite ± muscovite monzogranites. Microgranular enclaves of

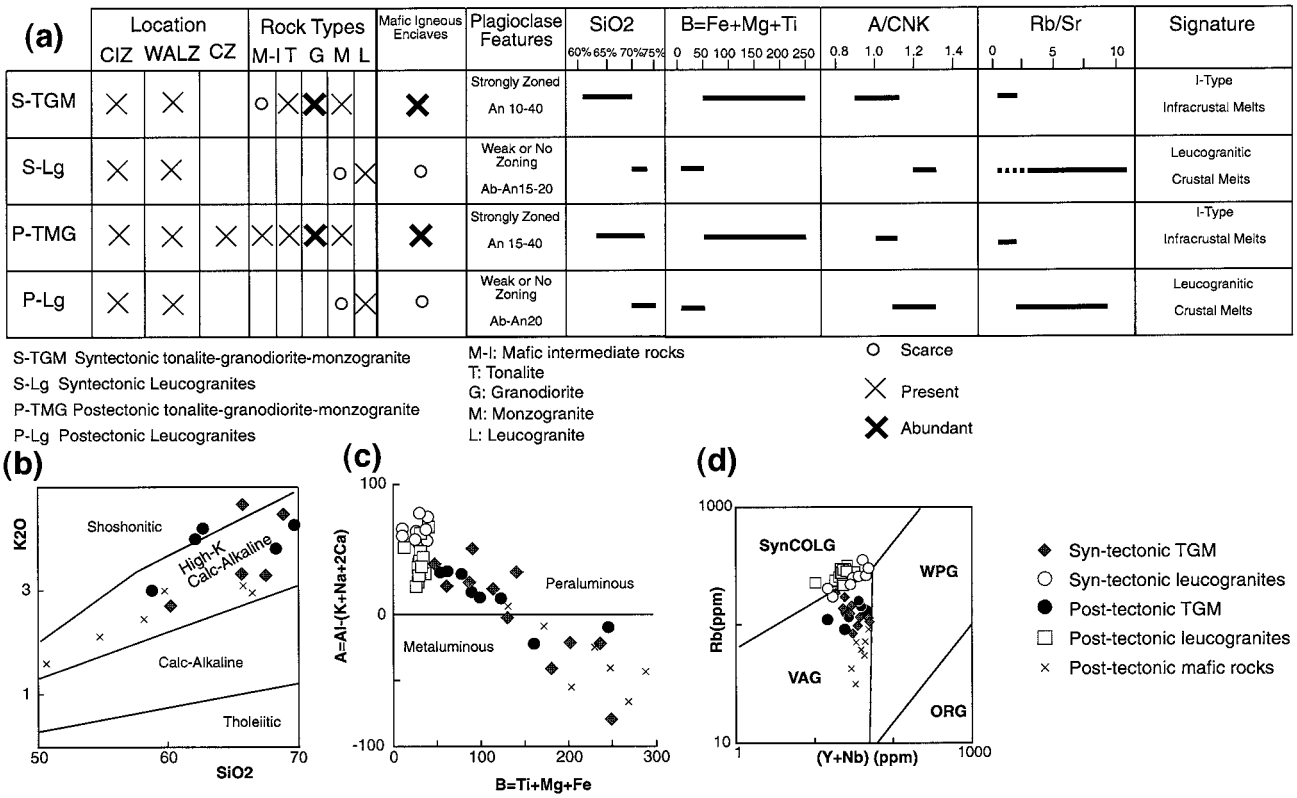

Fig. 2. (**a**) Summary of relevant petrologic and geochemical features of the studied granitoids. (**b**) SiO_2 v. K_2O diagram (field boundaries after Pecerillo & Taylor 1976) showing the high-K calc-alkaline nature of mafic-intermediate rocks, and syntectonic and post-tectonic TGM rocks. (**c**) A–B diagram of Debon & Le Fort (1983). (**d**) Rb v. Y+Nb (Pearce *et al.* 1984) tectonic discrimination diagram.

quartz-dioritic or tonalitic composition are frequent. SiO_2 contents range from *c.* 60% (tonalites) to 70%, with values up to 73% in monzogranitic facies. CaO ranges from *c.* 0.5 to 5% and MgO from *c.* 0.4 to 4%. Rb–Sr ratios are typically between 0.2 and 2 (Fig. 2). These rocks are slightly peraluminous (A/CNK $1 \approx 1.15$), although tonalitic rocks can be slightly metaluminous (A/CNK = 0.9–1) (Fig. 2) and monzogranitic rocks can be more peraluminous (A/CNK > 1.15). Rocks of this group generally display chemical features characteristic of high-K, I-type calc-alkaline granitoids (Fig. 2); (see Galán *et al.* 1996).

(ib) Syntectonic leucogranite plutons

Leucogranites are the volumetrically dominant syntectonic granitoid type in NW Iberia (Fig. 1). Field relationships indicate that these plutons were intruded during the D_2 deformation event, but after group (ia). Leucogranitoids of this group are two-mica (Ms>Bt) or muscovite leucomonzogranites, minor alkali feldspar granites and aplites. Microgranular igneous enclaves are lacking or very rare, and metasedimentary xenoliths are common. Geochemically, these leucogranites are characterized by silica contents mostly ranging from 70 to 73 SiO_2 wt% (Fig. 2), low Ca ($CaO \approx 0.3$–2%), low Mg ($MgO \approx 0.1$–0.7%) and a wide range of Rb/Sr ratios (0.2–11). These granites are strongly peraluminous with A/CNK ratios ranging between *c.* 1.2 and 1.3 and plot in the leucogranitoid field of the peraluminous domain in the A–B classification diagram of Debon & Lefort (1983) (Fig. 2).

(iia) Post-tectonic tonalite–granodiorite–monzogranite plutons

This petrological group is dominant in the post-tectonic association. There are biotite–amphibole tonalites, biotite ± amphibole granodiorites (common rock type) and biotite ± muscovite monzogranites (Fig. 1). Amphibole–biotite tonalites and quartz diorites appear as microgranular enclaves in most plutons of this group. These granitoids have SiO_2 contents ranging from *c.* 64 to 72 wt%, $CaO \approx 1.2$–3%, and $MgO \approx 0.7$–2% (Fig. 2). Rb/Sr ratios range from *c.* 0.3 to 2. Granitoids of this group are mildly peraluminous with A/CNK ratios ranging between *c.* 1 and 1.16 and straddle the Bt>Ms and Bt ± Amph fields of the peraluminous domain in the A–B classification diagram of Debon & Lefort (1983) (Fig. 2). As in the case of Group (ia), these rocks commonly display features characteristic of I-type high-K calc-alkaline granitoids (Fig. 2, see also Suárez *et al.* 1992).

(iib) Post-tectonic leucogranite plutons

Plutons of this group (Fig. 1) are two-mica (Ms>Bt) or muscovite leucomonzogranites, alkali feldspar granites and aplites. Microgranular mafic igneous enclaves are rare or lacking and metasedimentary xenoliths are common. Geochemically, these leucogranites are characterized by high silica contents ($SiO_2 \approx 70$–75%, Fig. 2), low Ca ($CaO \approx 0.7$–1.5%), low Mg (MgO<0.5%) and high Rb/Sr ratios (from 2 to 8). These granites are strongly peraluminous with A/CNK ratios ranging between *c.* 1.1 and 1.3 and plot in the leucogranitoid

field of the peraluminous domain in the A–B classification diagram of Debon & Lefort (1983) (Fig. 2).

In addition to the granitoids, there are some rare ultramafic and mafic to intermediate plutonic rocks either spatially associated to syn- and post-tectonic TGM intrusions, or as discrete small post-tectonic plutons in the Cantabrian and West Asturian Leonese zones. By volume, most of these rocks are post-tectonic, relatively more abundant in the Cantabrian Zone, and scarce in the West Asturian Leonese Zone and northwestern Central Iberian Zone. These rocks, which display a wide range of mineralogical and textural features, have been interpreted as mantle melts evolved through crystal fractionation and varying degrees of crustal contamination (Galán & Suárez 1989; Suárez *et al.* 1990, 1992; Galán *et al.* 1996) (see also Fig. 2).

Geochronological results

Sampling strategy

A suite of nine samples representative of the main types of granitoids and mafic rocks found in the West Asturian Leonese Zone was selected for U–Pb dating (Fig. 1). Based on their relationships with tectonic events and their geochemical features these samples are also broadly representative of the main granitoid types found in the autochthon of the NW Iberian Variscan collision belt (e.g. Capdevila *et al.* 1973; Corretgé 1983; Bellido *et al.* 1987).

Granitoids in the Boal–Ancares belt (Fig. 1) are post-tectonic and three samples representing the main petrological types were selected for dating: a quartz-diorite from the Porcia gabbro-diorite intrusion (PORJ-9); a monzogranite from the Boal granodiorite–monzogranite pluton (DJ-29); and a leucogranite from the Ancares leucogranite pluton (DJ-277). In the Lugo dome (Fig. 1), the Tojiza granodiorite–monzogranite pluton (sample TOJ-5) and the San Ciprián leucogranite pluton (sample VIV-7) were selected to constrain the age of intrusion of post-tectonic granitoids in this belt. Detailed structural work has shown that the Sarria and Hombreiro leucogranites (Fig. 1) were emplaced synkinematically with the Mondoñedo Nappe (Bastida *et al.* 1986; Aranguren & Tubía 1992). The Sarria leucogranite pluton (sample SA-4) was selected to date the intrusion age of these syn-D_2 leucogranites. The Penedo Gordo leucogranite pluton has been deformed by the extensional Vivero fault (Martínez Catalán 1985) and has been dated (sample PG-1) to provide an older age limit for the onset of the extensional motion of the Vivero fault. Finally, the granitoids forming part of the Vivero composite intrusion appear to be deformed by D_2 (Galán *et al.* 1996) and by the Vivero fault (Bastida *et al.* 1986). Monzogranite sample VGI-20 was selected to constrain the age of syntectonic TGM intrusions in the Lugo dome area and to further constrain the age span of D_2 deformation. Hornblendite sample VGI-6 was selected to test the possible non-coeval character of ultramafic rocks and granitoids in this composite intrusion.

Analytical techniques

Analytical work was carried out in the radiogenic isotope facility at Memorial University of Newfoundland. Heavy minerals were separated from crushed samples using standard density (Wilfley table, heavy liquids) and magnetic (Frantz Isodynamic separator) techniques. Selection of zircon and monazite fractions was carried out by hand-picking under a binocular microscope. Zircon was selected from the least magnetic Frantz split and monazite from a magnetic split at 1.0 A. All fractions, with the exception of those indicated in Table 1 were air abraded (Krogh 1982) to minimize lead-loss effects.

The zircon dissolution procedure follows Krogh (1973), save that the capacities of dissolution bombs and ion exchange columns, and volumes of reagents used are one order of magnitude less than those reported by Krogh (1973). Monazite fractions were dissolved in 6N HCl in Savillex containers, and U–Pb extraction was carried out by HBr column chemistry (Corfu & Scott 1986) with an additional purification of U. U and Pb were loaded together on a single Re filament with silica gel and H_3PO_4, and isotopic ratios measured on a Finnigan-MAT 262 mass spectrometer using up to four Faraday detectors in multicollection mode. Very small fractions or fractions with very small amounts of U and Pb were measured by peak jumping on a secondary electron multiplier (ion counting mode).

Total procedural blanks were generally 4–6 pg for Pb and <1 pg U for zircon analyses, and 15–20 pg Pb for monazite analyses. The Stacey & Kramers (1975) model was used to subtract initial common Pb in excess of the laboratory blank. Regression lines were calculated after Davis (1982) with intercept errors quoted at 95% confidence level. Decay constants are those of Jaffey *et al.* (1971).

U–Pb results

U–Pb (zircon and monazite) data obtained in this study are discussed in this section and presented in Table 1 and Fig. 3.

Porcia gabbro-diorite pluton (sample PORJ-9, Fig. 3a). Zircons from this sample are typically euhedral stubby prisms light to dark yellow in colour. Four fractions of these zircons were selected for analysis. Fraction Z3 yielded a concordant age of 295 ± 3 Ma, and two overlapping slightly discordant fractions (Z1 and Z4) have a $^{207}Pb/^{206}Pb$ age of 296 Ma. The age of crystallization of the Porcia gabbro-diorite intrusion is considered to be 295 ± 3 Ma. Discordant fraction Z2 is displaced to the right of the concordant point, and indicates the existence of an inherited component in the zircons of this pluton.

Boal monzogranite pluton (sample DJ-29, Fig. 3b). Three zircon and two monazite multigrain fractions were selected for analysis. Fractions Z1 and Z3 consist of short euhedral prisms transparent to light yellow in colour. These two fractions are highly discordant, whereas fraction Z2 composed of thin long prisms gave a much less discordant point. Monazite fractions consisting of subhedral grains yielded a concordant age of 292 ± 3 Ma. Since there is no tectonothermal event postdating the intrusion of the Boal pluton and zircon data are consistent with the concordant monazite age (lower intercept), the latter is considered to reflect the age of igneous crystallization of the intrusion.

Ancares leucogranite pluton (sample DJ-277, Fig. 3c). Three zircon and two monazite multigrain fractions were selected. Zircon fractions Z1 and Z3 consist of small euhedral stubby prisms transparent to light yellow in colour. Z2 consists of euhedral long and thin transparent prisms. As in the case of the Boal pluton all zircon fractions are discordant, the ones consisting of stubby prisms being the more discordant. The two monazite fractions, consisting of subhedral prisms yield a duplicated concordant to reverse discordant $^{207}Pb/^{235}U$ age of 289 ± 3 Ma. A regression using the three zircon fractions gives a lower intercept age of 285 Ma, although the probability of fit is low. The upper intercept average age of the inherited component is *c.* 1.7 Ga. As in the case of Boal, since there are no high-grade tectonothermal events after the intrusion of the pluton, the 289 ± 3 Ma monazite age is considered to represent the age of crystallization of this post-tectonic granite.

Tojiza granodiorite–monzogranite pluton (sample TOJ-5, Fig. 3d). Four zircon and two monazite multigrain fractions were selected for analysis. Fraction Z1 consisted of large euhedral equant prisms and is highly discordant. Fraction Z2 consisted

of long thin euhedral prisms and yielded a discordant age that probably reflects the combined effect of inheritance and lead loss. Fraction Z3 consisted of small euhedral prisms and yielded a concordant age of 295 ± 2 Ma. Fraction Z4 consists also of small euhedral prisms and yielded a slightly discordant (3.7%) age reflecting lead loss. The two monazite fractions consisting of small subhedral prisms yield points above concordia (reverse discordance, e.g. Parrish 1990) but with $^{206}Pb/^{238}U$ and $^{207}Pb/^{235}U$ ages ranging only from 294 to 297 Ma, overlapping Z3. Therefore, from the combined zircon and monazite data, the age of igneous crystallization is considered to be 295 ± 2.

San Ciprián leucogranite pluton (sample VIV-7, Fig. 3e). Three zircon and two monazite fractions were selected for analysis. Fractions Z1 and Z3 consisted of equant subhedral to euhedral small prisms and Z2 consisted of long thin prisms. Z1 and Z3 yielded highly discordant points reflecting a major inherited component. Z2 is less discordant and yielded a $^{207}Pb/^{206}Pb$ age of 318 Ma. The two monazite fractions consisting of relatively large subhedral to anhedral grains plot slightly above concordia and yielded a duplicated $^{207}Pb/^{235}U$ age of 286 ± 2 which is considered to represent the age of igneous crystallization of the leucogranite.

Vivero composite intrusion: hornblendite sample (VGI-6, Fig. 3f). Zircons from this sample are typically anhedral fragments light to dark brown in colour. A small number of grains were light pink to colourless. As seen in Table 1, the brown crystals have large amounts of Uranium (up to >10 000 ppm) whereas the transparent crystals have the lowest U contents.

Seven fractions (three single grains and four multigrain) were selected for analysis. Abraded multigrain fractions Z1, Z2, Z3 and Z4 are all discordant with $^{207}Pb/^{206}Pb$ ages between 281 and 295 Ma (Table 1). Single grain Z6 (transparent suhhedral) yielded a concordant point with a $^{206}Pb/^{238}U$ age of 293 Ma. Analysis of single grain Z5 (transparent anhedral) is less precise and plots below Z6 with a slightly older $^{207}Pb/^{206}Pb$ age. Fraction Z7 is a large non-abraded single brown zircon fragment and yielded a significantly more discordant point reflecting the strongest effect of lead loss. A regression using all seven fractions (11% probability of fit) gives an upper intercept age of 293^{+3}_{-2} Ma which agrees within error with the age of Z6. Therefore the upper intercept ge is considered to represent the age of igneous crystallization of the ultramafic rocks in the Vivero composite intrusion.

Vivero composite intrusion—monzogranite sample (VGI-20, Fig. 3g). Ten zircon and two monazite fractions were selected for analysis. Zircon fractions Z1, Z3 and Z10 consisted of small euhedral equant prisms, fraction Z2 consisted of long thin prisms and fractions Z4, Z5, Z6, Z7, Z8 and Z9 consisted of zircon needles (of which Z5, Z6 and Z9 were not abraded). All needle fractions except Z7 (slightly displaced to the right) are collinear and yield $^{207}Pb/^{206}Pb$ ages of 318–321 Ma (Table 1). A regression line using all needle fractions and a discordant monazite (M2) yields an upper intercept age of 323^{+9}_{-5} Ma with 16% probability of fit. Fraction Z7, consisting of slightly larger needles could reflect some minor inheritance. A regression line using the discordant fractions clearly containing inherited zircon (except Z2) yields a lower intercept age of 315 ± 2 Ma with 13.3% probability of fit. The upper intercept average age of the inherited component is *c.* 1.4 Ga. These two regression lines just meet at the limits of uncertainty. The correspondence of $^{207}Pb/^{206}Pb$ ages, well inside of analytical uncertainties, for five fractions of euhedral needle-like zircons indicates that these represent the best age estimate for the igneous crystallization of the monzogranites (upper intercept at 323^{+9}_{-5} Ma).

Monazite fractions consisted of subhedral crystals and yield two different ages. Fraction M1 yielded a concordant age of 295 ± 2, and fraction M2 is discordant but yielded a $^{207}Pb/^{206}Pb$ age of 323 Ma, collinear with the discordant needle zircon fractions. The meaning of the concordant age of monazite M1 (Table 1) is not clear, but this age corresponds to that of intrusion of basic magmas and granitoids into the middle and upper crust and represents a major late Variscan thermal event.

Penedo Gordo leucogranite pluton (sample PG-1, Fig. 3h). Eight zircon and two monazite multigrain fractions were selected for analysis. Z1 consisted of big equant euhedral prisms and yielded a highly discordant point reflecting inheritance. Fractions Z8 and Z3 consisted of small euhedral prisms and the rest of fractions consisted of zircon needles, of which Z5 was not abraded. A regression using Z2, Z3, Z4, Z6 and Z7, with consistent $^{207}Pb/^{206}Pb$ ages yields an upper intercept age of 317^{+9}_{-5} with a 42% probability of fit. Fraction Z8 is collinear within error with this regression. A regression using the previous fractions plus Z8 yields an upper intercept age of 320^{+10}_{-6} Ma, but the 317^{+9}_{-5} age is preferred since there is a consistent group of fractions with $^{207}Pb/^{206}Pb$ ages between 313 and 319 Ma (Table 1), and fraction Z8 could be slightly displaced to the right owing to minor inheritance.

Monazite fractions consisted of anhedral to subhedral grains and yielded overlapping $^{207}Pb/^{235}U$ ages of 293 ± 2 Ma, although both fractions plot slightly above concordia. As in the case of the Vivero monzogranites, the monazite age is younger than the age of igneous crystallization of the pluton and agrees within error with the concordant monazite age in the Vivero intrusion. Sample PG-1 was collected at the northern contact of the Penedo Gordo pluton, very close to the Vivero composite intrusion (Fig. 1), therefore we suggest that the intrusion of mafic–ultramafic rocks at *c.* 293 Ma may have provided the heat responsible for recrystallization of monazite.

Sarria leucogranite pluton (sample SA-4, Fig. 3i). Three zircon and two monazite multigrain fractions were selected for analysis. Fractions Z1 and Z3 consisted of euhedral equant small prisms and fraction Z2 of long prisms. All three fractions are highly discordant reflecting a major inherited component. The upper intercept average age of the inherited component is *c.* 1.7 Ga. The two monazite fractions consisting of subhedral to anhedral grains yielded a concordant age of 313 ± 2, which is considered to represent the age of crystallization of the pluton.

Discussion

Timing of plutonism

The U–Pb ages of granitoids in the West Asturian Leonese Zone provide new constraints on the age and duration of magmatic and tectonic events in this area and give new insights into the tectonothermal evolution of this section of the Iberian Variscan belt. These topics will be addressed in the following sections and their potential implications discussed in the light of pertinent geological and geochronologic data from neighbouring areas of the NW Iberian Variscan belt.

Table 1. *U–Pb analytical data*

Fraction*	Weight (mg)	U (ppm)	Pb_{rad} (ppm)†	Total Common Pb (pg)‡	Corrected atomic ratios§								Age (Ma)		
					206Pb/204Pb‡	$^{208}Pb/^{206}Pb$	$^{206}Pb/^{238}U$	2σ	$^{207}Pb/^{235}U$	2σ	$^{207}Pb/^{206}Pb$	2σ	$^{206}Pb/^{238}U$	$^{207}Pb/^{235}U$	$^{207}Pb/^{206}Pb$
PORJ-9 (postectonic diorite)															
Z1 eq euh dy	0.309	249	13.0	42	5330	0.2511	0.04650	14	0.3350	12	0.05225	6	293	293	297
Z2 lgp subh ly	0.221	251	13.3	25	6448	0.2543	0.04706	14	0.3411	10	0.05257	6	296	298	310
Z3 lrg eq euh ly	0.068	226	12.0	5	8311	0.2640	0.04687	18	0.3379	14	0.05229	10	295	296	298
Z4 eq euh ly	0.123	261	13.8	12	8020	0.2705	0.04646	16	0.3348	12	0.05226	8	293	293	297
DJ-29 (postectonic monzogranite)															
Z1 eq euh ly	0.222	1053	56.2	301	2713	0.0569	0.05547	16	0.4715	16	0.06166	6	348	392	662
Z2 lgp euh ly	0.093	1630	76.5	163	2727	0.1210	0.04652	16	0.3384	12	0.05276	6	293	296	319
Z3 eq euh ly	0.067	399	36.2	17	8685	0.1087	0.08809	26	1.0817	34	0.08906	8	544	744	1405
M1 eq subh	0.139	2492	585.7	287	3516	4.8219	0.04621	48	0.3330	32	0.05227	24	291	292	297
M2 eq subh	0.063	2776	692.9	132	3835	5.1728	0.04630	26	0.3322	20	0.05204	6	292	291	287
DJ-277 (postectonic leucogranite)															
Z1 eq euh tr	0.651	357	20.1	90	9179	0.0923	0.05650	18	0.4899	18	0.06288	6	354	405	704
Z2 lgp euh tr	0.145	497	23.0	61	3552	0.0750	0.04771	14	0.3644	12	0.05539	6	300	315	428
Z3 eq euh ly	0.015	156	9.8	4	2025	0.1384	0.06023	24	0.5580	28	0.06720	20	377	450	844
M1 eq subh	0.208	2324	565.4	291	4828	5.0339	0.04616	28	0.3293	18	0.05175	16	291	289	274
M2 eq subh	0.014	2234	653.0	20	4653	6.2977	0.04592	46	0.3296	32	0.05207	20	289	289	288
TOJ-5 (postectonic monzogranite)															
Z1 lrg eq euh tr	0.215	132	6.8	14	6076	0.1694	0.04870	24	0.3699	18	0.05509	6	307	320	416
Z2 lgp euh ly	0.054	137	7.0	6	3403	0.2109	0.04669	36	0.3419	24	0.05311	22	294	299	333
Z3 sml eq euh tr	0.020	167	8.3	7	1398	0.1794	0.04698	24	0.3371	18	0.05204	28	296	295	287
Z4 sml eq euh tr	0.683	166	8.2	53	6256	0.1799	0.04644	18	0.3356	14	0.05242	8	293	294	304
M1 sml eq subh	0.338	80	162.0	107	766	48.6342	0.04719	20	0.3376	18	0.05189	20	297	295	280
M2 sml eq subh	0.252	112	223.8	58	1438	48.1147	0.04702	18	0.3352	14	0.05170	14	296	294	272
VIV-7 (postectonic leucogranite)															
Z1 sml eq subh tr	0.157	862	48.8	15	33 542	0.0609	0.05862	22	0.5064	20	0.06265	6	367	416	696
Z2 lgp euh tr	0.027	2000	88.2	20	7981	0.0378	0.04702	18	0.3420	14	0.05276	6	296	299	318
Z3 smal eq euh ly	0.026	728	40.2	10	6582	0.0650	0.05731	26	0.4452	20	0.05634	14	359	374	466
M1 lrg eq anh	0.308	7332	1072.5	454	14 176	2.6666	0.04547	22	0.3247	16	0.05179	4	287	286	276
M2 lrg eq subh	0.346	7322	1062.5	554	13 021	2.6440	0.04539	24	0.3241	18	0.05179	4	286	285	276
VGI-6 (hornblendite)															
Z1 sml eq subh pk	0.056	3168	152.7	125	4035	0.1885	0.04516	16	0.3252	14	0.05223	12	285	286	295
Z2 frags br	0.300	5694	279.3	1167	4112	0.2249	0.04463	26	0.3209	20	0.05215	6	281	283	292
Z3 frags br	0.030	9120	427.2	483	1564	0.1964	0.04360	14	0.3129	12	0.05204	12	275	276	287
Z4 frags lbr	0.186	12 105	580.9	1428	4299	0.2356	0.04330	30	0.3109	22	0.05207	6	273	275	289
Z5 sgle subh tr	0.007	225	10.7	10	421	0.1507	0.04590	26	0.3320	48	0.05245	68	289	291	305
Z6 sgle subh pk	0.002	1004	48.1	7	1087	0.1440	0.04656	20	0.3357	18	0.05229	20	293	294	298
Z7 sgle frag na	0.016	10 222	457.0	106	3799	0.2699	0.03928	12	0.2821	10	0.05208	10	248	252	289
VGI-20 (syntectonic monzogranite)															
Z1 sml eq eu tr	0.159	702	35.7	38	9463	0.0848	0.05196	18	0.3887	14	0.05426	6	327	333	382
Z2 sml lgp euh	0.058	799	39.7	36	4145	0.0862	0.05069	18	0.3753	14	0.05371	6	319	324	359
Z3 sml eq euh tr	0.058	687	34.5	26	4835	0.1025	0.05053	22	0.3707	16	0.05320	10	318	320	338
Z4 needles	0.045	978	44.8	150	858	0.1127	0.04566	14	0.3326	14	0.05283	12	288	292	321
Z5 needles na	0.254	1274	56.6	941	1002	0.0763	0.04574	16	0.3328	14	0.05276	8	288	292	319
Z6 needles	0.130	1590	73.2	668	941	0.0739	0.04752	16	0.3460	14	0.05280	8	299	302	320
Z7 needles	0.040	1235	58.2	55	2700	0.0899	0.04789	16	0.3503	14	0.05305	8	302	305	331
Z8 needles	0.102	1486	68.8	161	2755	0.1093	0.04630	16	0.3371	12	0.05282	6	292	295	321
Z9 needles na	0.211	1603	73.0	1166	875	0.0701	0.04714	16	0.3428	16	0.05274	10	297	299	318
Z10 sml eq euh tr	0.117	1021	54.9	70	5787	0.0984	0.05417	18	0.4197	16	0.05618	6	340	356	460
M1 eq subh	0.195	5124	653.5	474	6216	2.0901	0.04694	20	0.3380	14	0.05222	4	296	296	295
M2 eq anh	0.020	5858	804.9	70	4409	2.3479	0.04671	18	0.3406	14	0.05288	6	294	298	324
PG-1 (syntectonic leucogranite)															
Z1 lrg eq euh tr	0.117	228	12.2	10	8558	0.1972	0.04973	16	0.3865	14	0.05637	10	313	332	467
Z2 needles	0.171	207	10.1	10	10 776	0.1456	0.04703	16	0.3415	10	0.05268	12	296	298	315
Z3 sml eq euh	0.013	151	7.3	9	633	0.1393	0.04750	24	0.3448	18	0.05264	20	299	301	313
Z4 needles	0.090	259	12.2	11	6068	0.1378	0.04600	22	0.3347	14	0.05278	14	290	293	319
Z5 needles na	0.275	439	19.0	173	1875	0.1266	0.04256	12	0.3074	10	0.05238	8	269	272	302
Z6 needles	0.097	418	18.2	8	13 682	0.1004	0.04391	18	0.3187	12	0.05265	12	277	281	314
Z7 needles	0.032	281	13.3	6	4228	0.1920	0.04419	22	0.3200	14	0.05253	18	279	282	308
Z8 sml eq euh	0.034	222	11.0	8	3000	0.1513	0.04806	36	0.3510	18	0.05298	34	303	305	328
M1 lrg eq subh	0.135	702	455.8	84	3338	14.9768	0.04671	20	0.3347	14	0.05198	10	294	293	284
M2 lrg eq anh	0.132	608	433.6	56	4169	16.5933	0.04662	16	0.3336	12	0.05191	8	294	292	281

Table 1. *Continued*

Fraction*	Weight (mg)	U (ppm)	Pb_{rad} (ppm)†	Total Common Pb (pg)‡	Corrected atomic ratios§								Age (Ma)		
					206Pb/204Pb‡	$^{208}Pb/^{206}Pb$	$^{206}Pb/^{238}U$	2σ	$^{207}Pb/^{235}U$	2σ	$^{207}Pb/^{206}Pb$	2σ	$^{206}Pb/^{238}U$	$^{207}Pb/^{235}U$	$^{207}Pb/^{206}Pb$
SA-4 (syntectonic leucogranite)															
Z1 sml eq subh	0.088	590	53.0	286	1025	0.0991	0.08858	30	0.9620	38	0.07876	12	547	684	1166
Z2 lgp euh	0.032	725	60.4	209	599	0.0814	0.08354	28	0.9041	38	0.07849	14	517	654	1159
Z3 sml eq euh	0.012	400	38.7	6	4963	0.1060	0.09561	38	0.9223	36	0.06996	16	589	664	927
M1 lrg eq subh lbr	0.160	3528	612.1	973	1825	2.9801	0.04972	24	0.3607	20	0.05262	6	313	313	312
M2 lrg eq subh br	0.184	3572	545.1	1375	1510	2.4880	0.04982	24	0.3609	18	0.05253	6	313	313	309

*Z, zircon, M, monazite; eq, equant; euh, euhedral; subh, subhedral; anh, anhedral, lgp, long prisms, lrg, large; frags, fragments; sgl, single grain; tr, transparent; ly, light yellow, pk, pink; br, brown,lbr, light brown; na, not abraded.
†Total radiogenic Pb after correction for blank, common Pb and spike.
‡Measured.
§Ratios corrected for fractionation, spike, 4–6 pg laboratory blank, initial common Pb (calculated with the Stacey & Kramers (1975) model for the age of the sample), and <1 pg U blank. Uncertainties (2σ) refer to the final digits.

The earliest Variscan granitoids in the West Asturian Leonese Zone are tonalite–granodiorite–monzogranite (TGM) plutons intruded synkinematically with D_2 at *c*. 325 Ma. The intrusion of these granitoids was followed shortly by the intrusion of leucogranite plutons at *c*. 320–310 Ma. This is consistent with field observations indicating that leucogranite magmatism post-dates the TGM magmatism (see Capdevila *et al*. 1973; Martínez Catalán 1985; Bastida *et al*. 1986). Therefore, the intrusion of the syntectonic association in the West Asturian Leonese Zone took place in a time span of *c*. 15 Ma, from *c*. 325 Ma to *c*. 310 Ma.

The post-tectonic magmatic association, dominated by TGM intrusions and associated mafic–intermediate rocks, was emplaced at *c*. 295–290 Ma. It is very important to note that the ultramafic rocks associated with the Vivero granitoids yielded an age of *c*. 293 Ma (Fig. 3f) and therefore they are not coeval with the spatially associated syntectonic granitoids (*c*. 325 Ma, Fig. 3g) but intruded them during the post-tectonic magmatic event. Lesser amounts of leucogranites also form part of the post-tectonic association and were emplaced at 290–285 Ma. This suggests that post-tectonic leucogranite magmatism in the West Asturian Leonese Zone is slightly younger than the post-tectonic TGM plutons and associated mafic-intermediate rocks.

These data illustrate the episodic nature of Variscan magmatism in the West Asturian Leonese Zone. Each magmatic episode is characterized by granitoids with distinct features (e.g. relative volumes of different rock types) and has a duration on the scale of 10–15 Ma. The episodic nature of Variscan magmatism has also been revealed in other areas of Western Europe where precise U–Pb data are available (e.g. Schaltegger 1997; Dias *et al*. 1998).

Age of deformation events

The U–Pb ages of granitoids in the West Asturian Leonese Zone provide new constraints on the age and duration of the main deformation events in the area. The ages reported in this study indicate that the D_2 deformation episode in the West Asturian Leonese Zone (whose main associated structure is the basal thrust of the Mondoñedo Nappe) covers a minimum time span of about 15 Ma, from *c*. 325 Ma (age of the Vivero synkinematic TGM intrusion) to *c*. 310 Ma (constrained by the age of the Sarria leucogranite pluton). These U–Pb constraints on the age of the D_2 event are consistent with the $^{40}Ar/^{39}Ar$ ages for the peak of D_2 in the West Asturian Leonese Zone (*c*. 315–330 Ma) reported by Dallmeyer *et al*. (1997).

The age of the Penedo Gordo leucogranite pluton provides an upper age limit for the xtensional motion of the Vivero fault at *c*. 317 Ma. This datum is consistent with structural and metamorphic studies which indicate the overlap in timing of the Mondoñedo thrust and the extensional Vivero fault (Martínez Catalán 1985; Aranguren & Tubía 1992; Reche *et al*. 1998). In addition, Aranguren & Tubía (1992) provided microstructural evidence indicating that the extensional motion of the Vivero fault might have been initiated during or shortly after the intrusion of these leucogranites. Therefore an age of *c*. 317 Ma is suggested as an estimate for the onset of extensional collapse in this domain of the Iberian Variscan belt. This age constraint for syn-convergence extension suggests that this event is slightly younger in the West Asturian Leonese Zone than in the adjacent Central Iberian Zone, where syn-convergence extension is interpreted to have occurred between *c*. 335 and 320 Ma on the basis of monazite/titanite U–Pb dating of fabrics (Valverde-Vaquero *et al*. 1995). Finally, the intrusion ages of post-tectonic granitoids in the West Asturian Leonese Zone indicate that the main deformation events in this zone ended before *c*. 295 Ma.

Spatial distribution, relative volume and timing of Variscan magmatism in NW Iberia

The distribution of main granitoid types in the autochthon of the NW Iberian Variscan belt is illustrated in Fig. 4. From this figure, it can be observed that the dominant rock type in the syntectonic association is leucogranite (Fig. 4a,b) (>75% in volume of the present day outcrop), whereas the TGM intrusions are a relatively minor feature. Figure 4a also shows that the syntectonic TGM intrusions define a plutonic belt that is roughly coincident with the 'domain of recumbent folds' in the Central Iberian Zone (Díez Balda *et al*. 1990) (Fig. 1). This domain is interpreted to represent the area where maximum crustal thickness was attained during the Variscan collision. Figure 4b shows that the syntectonic leucogranite plutonic belt is significantly wider than the TGM belt. Finally, Fig. 4(a & b) illustrates the absence of syntectonic intrusions in the foreland

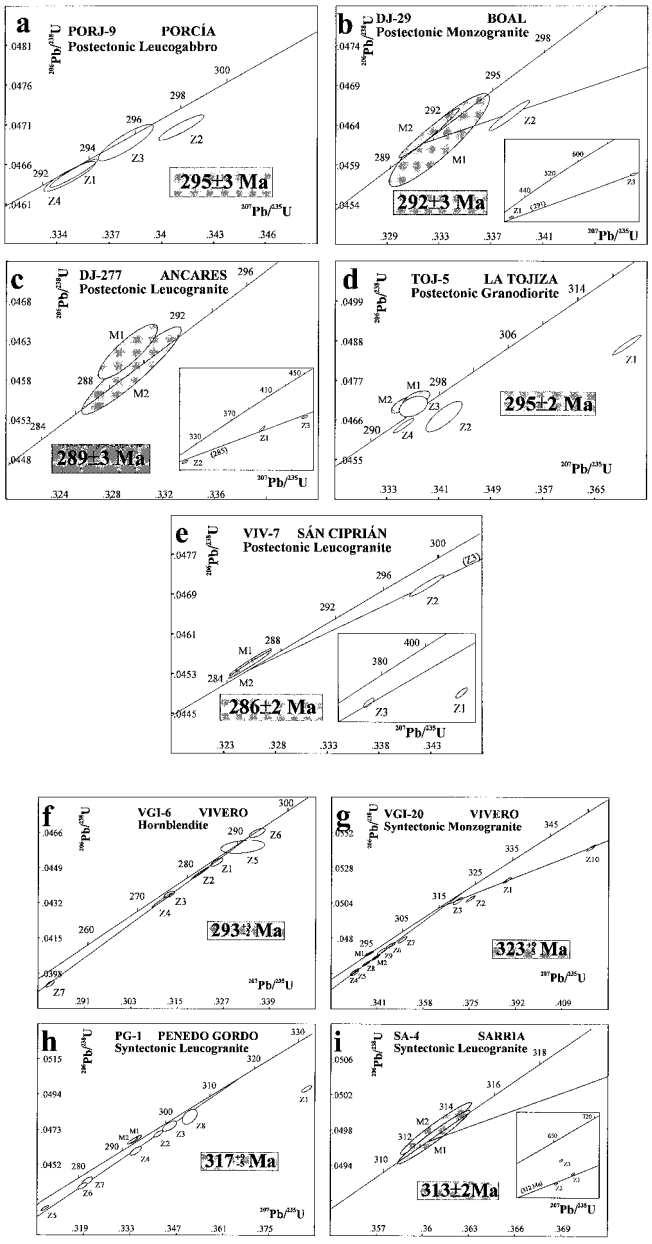

Fig. 3. U–Pb Concordia plots. Ellipses represent 2σ uncertainties. Shaded ellipses correspond to monazite fractions. Sample locations indicated in Fig. 1.

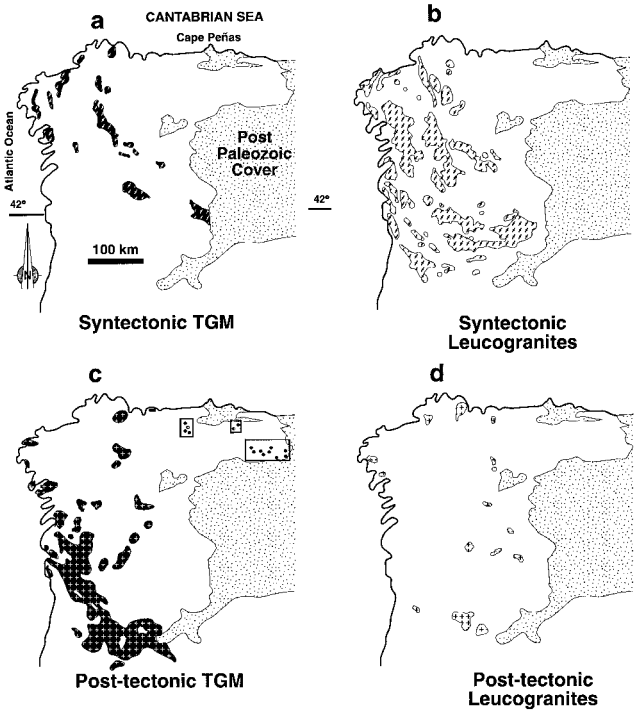

Fig. 4. Maps showing the spatial distribution of the main granitoid groups in the Variscan belt of NW Iberia (modified after Corretgé 1983). Squares in (c) represent areas with abundant small plutonic outcrops in the Cantabrian Zone.

of the Iberian Variscan collision belt (Cantabrian Zone) and in most of the West Asturian Leonese Zone (see also Fig. 1).

In the post-tectonic association the relative volume of granitoids is reversed and the TGM intrusions are the dominant granitoid type (Fig. 4c), and leucogranites are a minor feature (Fig. 5d). With regard to Fig. 4(c,d), three important observations can be made: (i) unlike the syntectonic granitoids, the post-tectonic TGM intrusions appear in all zones of the NW Iberian Variscan belt, and are the first igneous rocks to appear in the foreland (Cantabrian Zone) along with mafic-intermediate rocks; (ii) leucogranites are practically absent in the Cantabrian Zone; (iii) there is an increase in the exposed volume of post-tectonic TGM intrusions from NE to SW. The presence of granitoids in the Cantabrian Zone (Fig. 4c) is remarkable because it reveals the existence of significant plutonism in a foreland area characterized by thin-skinned tectonics without significant crustal thickening, at variance with foreland areas in other orogenic belts.

With regards to the ages of other granitoids in the NW Iberian Variscan belt, although high-precision U–Pb dating is still scarce, the age of the earliest syntectonic TGM plutons (Fig. 4a) seems to vary from *c*. 350–340 Ma in the Central Iberian Zone (Bellido *et al*. 1992; Gallastegui 1993) to *c*. 325 Ma in the West Asturian Leonese Zone (this study). The age of syntectonic leucogranites is not well constrained in the Central Iberian Zone. Available Rb-Sr isochrons indicate that the age of these granitoids ranges from *c*. 340–320 Ma in the domain of vertical folds (Serrano Pinto *et al*. 1987; Reavy *et al*. 1991; Beetsma 1995) to *c*. 325–315 Ma in the domain of recumbent folds (Capdevila & Vialette 1970; Priem & Den Tex 1984; Ortega 1995). In the West Asturian Leonese Zone, we have obtained U–Pb ages for two syntectonic leucogranites: the Penedo Gordo pluton (*c*. 317 Ma); and the Sarria pluton (*c*. 313 Ma). The apparent age migration of the syntectonic leucogranite magmatism from the Central Iberian Zone to the West Asturian Leonese Zone is consistent and roughly coeval with the age migration of syn-convergence extension in this section of the Variscan belt (Valverde *et al*. 1995; Dallmeyer *et al*. 1997).

The ages of post-tectonic granitoids are generally between *c*. 290 and 295 Ma in the Cantabrian Zone (Valverde *et al*. 1999), the West Asturian Leonese Zone (this study) and the domain of recumbent folds of the Central Iberian Zone (Serrano Pinto *et al*. 1987; Valverde *et al*. 1995; Villaseca *et al*. 1995; Yenes *et al*. 1996). U–Pb ages on post-tectonic granitoids

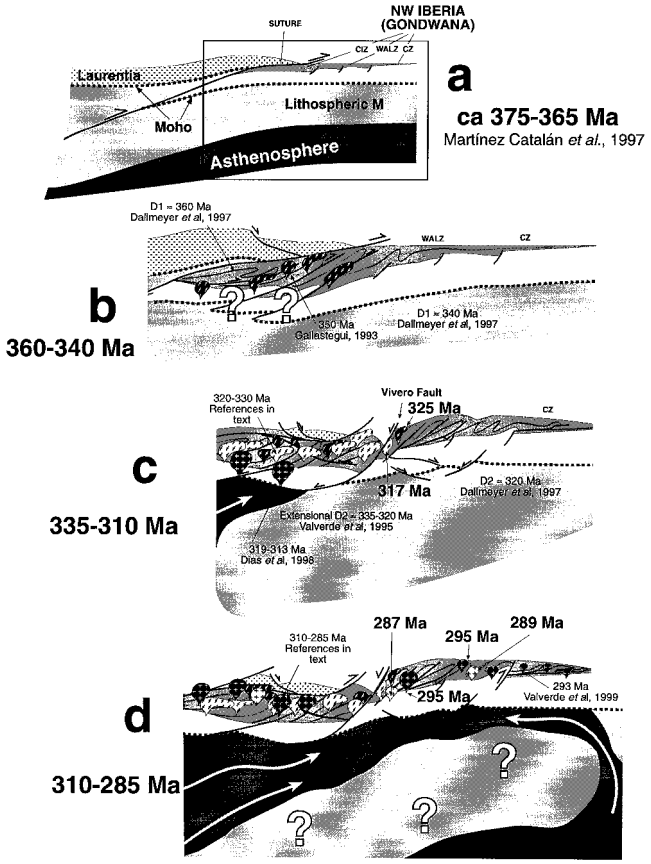

Fig. 5. Proposed tectonic evolution of the NW Iberian Variscan belt. Simplified sketch of the general cross section based in previous works by Martínez Catalán *et al.* (1990, 1996, 1997) and Pérez Estaún *et al.* (1991). (**a**) Scenario preceding the genesis of the syntectonic association in the autochthonous of NW Iberia. (**b, c**) Tentative scenario for the genesis of the syntectonic association. (**d**) Scenario for the genesis of the post-tectonic association.

from this study suggest that in the West Asturian Leonese Zone, the TGM intrusions (*c.* 290–295 Ma) pre-date the intrusion of the scarcer peraluminous leucogranites (*c.* 285–290 Ma). As noted above, the TGM post-tectonic intrusions become progressively more abundant andvoluminous from NE (Cantabrian Zone) to SW (domain of vertical folds of the Central Iberian Zone) (Fig. 4c). Within this latter area (North Portugal), a recent study by Dias *et al.* (1998) has provided new U–Pb zircon and monazite ages for these granitoids. According to this study, early (volumetrically scarce) post-tectonic TGM magmatism occurred between *c.* 319 and 313 Ma and was followed by voluminous TGM and mafic plutonism between *c.* 311 and 290 Ma. Subordinate leucogranites in the same area have younger ages between *c.* 300 and 280 Ma.

Tectonics and a hypothesis for Variscan magmatism

Based upon the geochronological data presented in this study and on the general framework of NW Iberian Variscan magmatism outlined in the previous section, we now examine the relationship of the magmatic episodes with models for the tectonic evolution of the Variscan orogen in NW Iberia (Pérez Estaún *et al.* 1991; Martínez Catalán *et al.* 1996, 1997). According to these models, granitoids in the autochthonous zone of the NW Iberian Variscan belt were generated in a setting of eastward migrating intracontinental deformation. This event followed the closure of the Rheic ocean, the subduction of the outer edge of Gondwana (*c.* 375 Ma) and the westward underthrusting of Gondwanan crust (Martínez Catalán *et al.* 1997).

The proposed sequence of events is illustrated in Fig. 5. Westward underthrusting of Gondwanan lithosphere occurred at *c.* 375–365 Ma (Fig. 5a) (Martínez Catalán *et al.* 1996, 1997). In the autochthon of NW Iberia, there is no significant record of magmatic activity related to this stage. The oldest granitoids in the autochthon of NW Iberia are the TGM plutons emplaced at *c.* 350–340 Ma in the Central Iberian Zone (Figs 4a, 5b). Field observations indicate that these plutons cut D_1 structures and are deformed by D_2 (see Gallastegui 1993), in agreement with the $^{40}Ar/^{39}Ar$ ages of D_1 (*c.* 360 Ma) and D_2 (*c.* 343 Ma) fabrics in the same domain (Dallmeyer *et al.* 1997). In the West Asturian Leonese Zone, the intrusion of syntectonic TGM granitoids took place at *c.* 325 Ma (this study, Fig. 5c). Field observations also indicate that the intrusions are roughly coeval with D_2, in agreement with $^{40}Ar/^{39}Ar$ ages of D_2 fabrics (*c.* 330–315 Ma; Dallmeyer *et al.* 1997). Therefore, the migration of ages of the metamorphism across the orogen is consistent with the migration in age of the syntectonic TGM granitoids. The syntectonic TGM plutons have petrological and isotopic signatures consistent with a mixed mantle-lower crust genesis in both the West Asturian Leonese Zone and in the Central Iberian Zone (Gallastegui 1993; Beetsma 1995; Galán *et al.* 1996). Early Variscan (*c.* 360–350 Ma) mantle melting and concomitant underplating of the lower crust is one of the possible mechanisms that could have triggered the generation of the syntectonic TGM granitoids. Although there is no solid evidence to support this hypothesis, it should be noted that mafic underplating of the Variscan lower crust is believed by some authors to have started at *c.* 360 Ma (Downes *et al.* 1990).

With regard to the syntectonic leucogranites there is evidence indicating that they were intruded during syn-convergence extension related to the collapse of the orogenic belt (Aranguren & Tubía 1992; Escuder Viruete *et al.* 1994; Díez Balda *et al.* 1995; Martínez Catalán *et al.* 1996; Ayarza *et al.* 1998). In the Central Iberian Zone the age of these granitoids (*c.* 340–320 Ma) fits ages of extensional fabrics related to this event (335–320 Ma, Valverde-Vaquero *et al.* 1995). In the West Asturian Leonese Zone, the Penedo Gordo pluton, intruded at *c.* 317 Ma and deformed by the extensional Vivero fault (Fig. 5c), seems to indicate a younger age for the onset of extensional structures in the West Asturian Leonese Zone, which is consistent with proposed rates of migration of deformation across the orogenic belt (Dallmeyer *et al.* 1997). Given the apparent synchronicity of leucogranite production and extensional collapse of the orogenic belt, a potential mechanism to explain the genesis of these leucogranites is decompression melting of the middle-upper crust as a consequence of the development of gravitationally induced extensional detachments (Fig. 5c) (see Zeitler & Chamberlain 1991). This hypothesis is consistent with the evolved-crust geochemical signatures displayed by many of these leucogranites (e.g. Beetsma 1995; Ortega 1995; Dias *et al.* 1998).

As regards the post-tectonic association, the intrusion of most plutons occurred in a time span of *c.* 295–285 in the Cantabrian Zone, West Asturian Leonese Zone and northern Central Iberian Zone. However, recent U–Pb data indicate

that further south in the Central Iberian Zone the volumetrically dominant TGM plutonism started at *c.* 311 Ma (Dias *et al.* 1998). The following aspects are of key importance for the interpretation of post-tectonic dominantly TGM-type magmatism: (1) this event occurs at orogenic belt scale and is represented from the foreland to the innermost part of the orogen; (2) the post-tectonic magmatic event occurs in a relatively short time span (*c.* 10 Ma, from 295 to 285) in the Cantabrian, West Asturian Leonese and northern Central Iberian Zones, and started some 10–15 Ma earlier in the most internal zones of the belt (Fig. 5c); (3) petrological, geochemical and isotopic features of these granitoids point to a genesis by melting of the lower crust with varying degrees of involvement of mantle derived melts (Galán & Suárez 1989; Suárez *et al.* 1992; Valverde-Vaquero 1992; Dias & Leterrier 1994; Beetsma 1995; Moreno Ventas *et al.* 1995). To explain the genesis of voluminous (Fig. 4c) high-temperature melts (biotite ± amphibole granodiorites plus mafic intermediate rocks) over an orogen scale area several hundred kilometers wide, an extremely efficient heat source must have been involved. In a post-collisional context, a likely mechanism to trigger such a voluminous and widespread magmatic event is delamination of the lithosphere (e.g. Nelson 1992; Turner *et al.* 1992; Collins 1994). Arguments in favour of such process are: (a) the geochemical signatures indicating a mixed mantle–crust origin at orogenic belt scale (Cantabrian, Western Asturian Leonese and Central Iberian Zones) (references above); (b) the existence of relatively abundant mafic–intermediate rocks and granodiorites in the foreland basin (Cantabrian Zone); (c) delamination is also consistent with the metamorphic history of the NW Iberian Variscan belt, wherein an earlier higher pressure metamorphic event is overprinted by a later low pressure-high temperature event (Collins 1994); (d) the older age of post-tectonic magmatism in the Central Iberian Zone (Dias *et al.* 1998) is consistent with the initiation of delamination under the internal zones of the orogenic belt, where crustal thickening and subsequent extensional collapse occurred earlier than in areas situated towards the foreland (Fig. 5c). In the present case, delamination might have started between *c.* 319 and 310 Ma under the Central Iberian Zone (Fig. 5c), some 50 Ma after the main collision event (Fig. 5a), and reached its acme between 300 and 290 Ma under the whole belt (Fig. 5d). This time framework is in agreement with postulated time scales for mechanical thinning of lithospheric mantle beneath orogenic belts (e.g. Nelson 1992). Finally, it should be noted that this hypothesis has also been proposed by authors working in other areas of the European Variscides based upon geochemical studies of granitoids (see Pin & Duthou 1990; Schaltegger 1997) and lower crustal granulites (Vielzeuf & Pin 1989; Pin 1990).

Corollary

The granitoid chronology and typology fit into the overall scheme of tectonometamorphic evolution of this section of the Variscan orogen and are consistent with geological observations, spatial distrubution and fabric age data. U–Pb geochronology highlights the episodic character of Variscan granitoid magmatism in the West Asturian Leonese Zone. The syntectonic tonalite–granodiorite–monzogranite intrusions are the earliest granitoids in the NW Iberian Variscan belt. They were generated synchronously with the peak of crustal thickening as a consequence of lower crustal melting possibly induced by early mafic underplating of the Variscan lower crust. The voluminous syntectonic leucogranite magmatism in the authochthonous of the NW Iberian Variscan belt was generated synchronously with the development of synconvergence extensional structures. Decompression melting of the crust triggered by extensional collapse may explain the origin of the leucogranites. Post-tectonic magmatism is dominated by tonalite-granodiorite-monzogranite intrusions and we propose that it was produced as a consequence of the high heat flow generated by delamination of the lithosphere and upwelling of asthenospheric mantle.

J.F.S. wishes to acknowledge a postdoctoral grant from the Spanish Ministry of Education. R. Hicks, P. Horan, M. Tubrett, P. King and L. Hewa are kindly acknowledged for their help with laboratory work. G. Galán is kindly acknowledged for valuable field guidance and advise during sampling of the Vivero intrusion. J. R. Martínez Catalán is thanked for valuable advice in planning the sampling strategy. Reviews by C. Pin, U. Schaltegger, L. G. Corrtegé and R. Parrish contributed to improve the manuscript. Financial support for this research was provided by NSERC operating grants to G.R. Dunning and G.A. Jenner, an NSERC Major Facilities Access grant for the ICP-MS facility and a NATO travel grant to J.F.S., G.A.J. and F. Bea. Additional financial support to G.G.A. was provided by DGIYCT project PB96-1452-C03-02.

References

Aranguren, A. & Tubia, J.M. 1992. Structural evidence for the relationship between thrusts, extensional faults and granite intrusions in the Variscan belt of Galicia (Spain). *Journal of Structural Geology*, **14,** 1229–1237.

Ayarza, P., Martínez Catalán, J.R., Gallart, J., Pulgar, J.A. & Doñobeitia, J.J. 1998. Estudio sísmico de la cortezaIbérica Norte 3.3: A seismic image of the Variscan crust in the hinterland of the NW Iberian massif. *Tectonics*, **17,** 171–186.

Bastida, F., Martínez Catalán, J.R. & Pulgar, J.A. 1986. Structural, metamorphic and magmatic history of the Mondoñedo nappe (Hercynian belt, NW Spain). *Journal of Structural Geology*, **8,** 415–430.

Beetsma, J.J. 1995. *The late Proterozoic/Paleozoic and Hercynian crustal evolution of the Iberian massif, N Portugal*. PhD thesis, Free Universiteit Amsterdam.

Bellido, F., González Lodeiro, F., Klein, E., Martínez Catalán, J.R. & Pablo Macía, J.G. 1987. *Las rocas graníticas hercínicas del Norte de Galicia y occidente de Asturias*. Mememorias del Instituto Geológico y Mininero de España, **101**.

Bellido, F., Brandle, J.L., Lasala, M. & Reyes, J. 1992. Consideraciones petrológicas y cronológicas sobre las rocas graníticas Hercínicas de Galicia. *Cuadernos del Laboratorio Geológico de Laxe*, **17,** 241–261.

Capdevila, R. & Vialette, Y. 1970. Estimation radiométrique de l'âge de la deuxième phase tectonique hercynienne en Galice Moyenne (Nord-Ouest de l'Espagne). *Comptes Rendues de l'Académie des Sciences de Paris*, **270,** 2527–2530.

——, Corretgé, L.G. & Floor, P. 1973. Les granitoides varisques de la Meseta Ibérique. *Bulletin de la Societé Géologique de France*, **15,** 209–228.

Collins, W.J. 1994. Upper- and middle-crustal response to delamination, an example from the Lachlan foldbelt, eastern Australia. *Geology*, **22,** 143–146.

Corfu, F. & Scott, G.M. 1986. U-Pb ages for late magmatism and regional deformation in the Shebandowan belt, Superior Province, Canada. *Canadian Journal of Earth Sciences*, **23,** 1075–1082.

Corretgé, L. G. 1983. Las rocas graníticas y granitoides del Macizo Ibérico. *In*: Comba, J. A. (ed.) *Geología de España. Libro Jubilar JM Rios*. IGME, **1,** 115–128.

——, Suárez, O. & Galán, G. 1990. West Asturian-Leonese Zone. Igneous rocks. *In*: Dallmeyer, R.D. & Martínez García, E. (eds) *Pre-Mesozoic Geology of Iberia*. Springer Verlag, 115–128.

Dallmeyer, R.D., Martínez Catalán, J.R., Arenas, R., Gil Ibarguchi, J.I., Gutiérrez Alonso, G., Farias, P., Bastida, F. & Aller, J. 1997. Diachronous Variscan tectonothermal activity in the NW Iberian Masif: Evidence from $^{40}Ar/^{39}Ar$ dating of regional fabrics. *Tectonophysics*, **277,** 307–337.

Davis, D.W. 1982. Optimum linear regression and error estimation applied to U–Pb data. *Canadian Journal of Earth Sciences*, **19,** 2141–2149.

Debon, F. & Le Fort, P. 1983. A chemical-mineralogical classification of common plutonic rocks and associations. *Transactions of the Royal Society of Edinburgh*, **73,** 135–149.

Dias, G. & Leterrier, J. 1994. The genesis of felsic-mafic plutonic associations: a Sr and Nd isotopic study of the Hercynian Braga Granitoid massif (Northern Portugal). *Lithos*, **32,** 207–223.

——, ——, Mendes, A., Simoes, P.P. & Bertrand, J.M. 1998. U-Pb zircon and monazite geochronology of post-collisional Hercynian granitoids from the Central Iberian zone (northern Portugal). *Lithos*, **45,** 349–369.

Diez Balda, M.A., Martínez Catalán, J.R. & Ayarza, P. 1995. Syn-collisional extensional collapse parallel to the orogenic trend in a domain of steep tectonics: the Salamanca detachment zone (Central Iberian Zone, Spain). *Journal of Structural Geology*, **17,** 163–182.

——, Vegas, R. & González Lodeiro, F. 1990. Central Iberian zone: Authochthonous sequences. Structure. *In*: Dallmeyer, R.D. & Martínez García, E. (eds) *Pre-Mesozoic Geology of Iberia*. Springer Verlag, 171–188.

Downes, H., Dupuy, C. & Leyreloup, A.F. 1990. Crustal evolution of the Hercynian belt of western Europe: evidence from lower crustal xenoliths (French Massif Central). *Chemical Geology*, **83,** 209–231.

Escuder Viruete, J., Arenas, R. & Martínez Catalán, J.R. 1994. Tectonothermal evolution associated with Variscan crustal extension in the Tormes Gneiss dome (NW Salamanca, Iberian Massif, Spain). *Tectonophysics*, **238,** 117–138.

Fernández-Suárez, J. 1994. *Petrología de los granitos peralumínicos y metamorfismo de la banda Boal-Los Ancares*. PhD thesis, University of Oviedo.

Fernández-Suárez, J., Gutiérrez-Alonso, G., Jenner, G.A. & Jackson, S.E. 1998. Geochronology and geochemistry of the Pola de Allande granitoids (northern Spain). Their bearing on the Cadomian/Avalonian evolution of NW Iberia. *Canadian Journal of Earth Sciences*, **35,** 1439–1453.

Galán, G. & Suárez, O. 1989. Cortlanditic enclaves associated with calc-alkaline granites from Tapia-Asturias (Hercynian Belt, northwestern Spain). *Lithos*, **23,** 233–245.

——, Pin, C. & Duthou, J.L. 1996. Sr-Nd isotopic record of multi-stage interactions between mantle-derived magmas and crustal components in a collision context. The ultramafic-granitoid association from Vivero (Hercynian belt, NW Spain). *Chemical Geology*, **131,** 67–91.

Gallastegui, G. 1993. *Petrología del macizo granodioritico de Bayo-Vigo (Pontevedra, España)*. PhD thesis, University of Oviedo.

Jaffey, A.H., Flynn, K.F., Glendenin, L.E., Bentley, W.C. & Essling, A.M. 1971. Precission measurements of half-lives and specific activities of ^{235}U and ^{238}U. *Physical Reviews C: Nuclear Physics*, **4,** 1889–1906.

Krogh, T.E. 1973. A low contamination method for hydrothermal decomposition of zircon and extraction of U and Pb for isotopic age determination. *Geochimica et Cosmochimica Acta*, **37,** 485–494.

—— 1982. Improved accuracy of U-Pb ages by the creation of more concordant systems using an air abrasion technique. *Geochimica et Cosmochimica Acta*, **46,** 637–649.

Martínez Catalán, J.R. 1985. Estratigrafía y estructura del Domo de Lugo (Sector Oeste de la zona Asturoccidental-leonesa). *Corpus Geologicum Gallaeciae*, **2,** 1–291.

——, Arenas, R., Díaz García, F. & Abati, J. 1997. Variscan accretionary complex of northwest Iberia: Terrane correlation and succession of tectonothermal evens. *Geology*, **25,** 1103–1106.

——, ——, ——, Rubio Pascual, F.J., Abati, J. & Marquínez, J. 1996. Variscan exhumation of a subducted Paleozoic continental margin: the basal units of the Ordenes complex, Galicia, NW Spain. *Tectonics*, **15,** 106–121.

——, Pérez Estaún, A., Bastida, F. & Pulgar, J.A. 1990. West Asturian-leonese Zone. Structure. *In*: Dallmeyer, R.D. & Martínez García, E. (eds) *Pre-Mesozoic Geology of Iberia*. Springer Verlag, 103–114.

Martínez, F. J., Carreras, J. & Arboleya, M. L. 1996. Structural and metamorphic evidence of local extension along the Vivero fault coeval with bulk crustal shortening in the Variscan chain. *Journal of Structural Geology*, **18,** 61–73.

——, Julivert, M., Sebastián, A., Arboleya, M.L. & Gil Ibarguchi, J.I. 1988. Structural and thermal evolution of high-grade areas in the northwestern parts of the Iberian Massif. *American Journal of Science*, **288,** 969–996.

Moreno Ventas, I., Rogers, G. & Castro, A. 1995. The role of hybridization in the genesis of of Hercynian granitoids in the Gredos Massif, Spain: inferences from Sr-Nd isotopes. *Contributions to Mineralogy and Petrology*, **120,** 137–149.

Nelson, K.D. 1992. Are crustal thickness variations in old mountain belts like the Appalachians a consequence of lithospheric delamination? *Geology*, **20,** 488–502.

Ortega, A. 1995. *Estudio petrogenético del granito sincinemático de dos micas de la Espenuca (La Coruña)*. PhD Thesis, University of the Basque Country.

Parrish, R.R. 1990. U-Pb dating of monazite and its application to geological problems. *Canadian Journal of Earth Sciences*, **27,** 1431–1450.

Pearce, J.A., Harris, N.B.W. & Tindle, A.G. 1984. Trace element discrimination diagrams for the tectonic interpretation of granitic rocks. *Journal of Petrology*, **25,** 956–983.

Peccerillo, A. & Taylor, S.R. 1976. Geochemistry of Eocene calc-alkaline volcanic rocks from the Kastamonu area, northern Turkey. *Contributions to Mineralogy and Petrology*, **58,** 63–81.

Pérez Estaún, A., Bastida, F., Martínez Catalán, J.R., Gutiérrez Marco, J.C., Marcos, A. & Pulgar, J.A. 1990. West Asturian-Leonese Zone. Stratigraphy. *In*: Dallmeyer, R.D. & Martínez García, E. (eds) *Pre-Mesozoic Geology of Iberia*. Springer Verlag, 92–102.

——, Martínez Catalán, J.R. & Bastida, F. 1991. Crustal thickening and deformation sequence in the footwall to the suture of the Variscan belt of northwest Spain. *Tectonophysics*, **191,** 243–253.

Pin, C. 1990. Evolution of the lower crust in the Ivrea zone: a model based on isotopic and geochemical data. *In*: Vielzeuf, D. & Vidal, P. (eds) *Granulites and crustal evolution*. Kluwer Academic Press, 87–110.

—— & Duthou, J.L. 1990. Sources of Hercynian granitoids from the French Massif Central: inferences from Nd isotopes and consequences for crustal evolution. *Chemical Geology*, **83,** 281–296.

Priem, H.N.A. & Den Tex, E. 1984. Tracing crustal evolution in the NW Iberian Peninsula through the Rb-Sr and U-Pb systematics of Paleozoic granitoids: A review. *Physics of Earth and Planetary Interiors*, **35,** 121–130.

Reavy, R.J., Stephens, W.E., Fallick, A.E., Halliday, A.N. & Godinho, M.M. 1991. Geochemical and isotopic constraints on petrogenesis: The Serra da Freita pluton, a typical granite body from the Portuguese Hercynian collision belt. *Geological Society of America Bulletin*, **103,** 392–401.

Reche, J., Martínez, F.J., Arboleya, M.L., Dietsch, C. & Briggs, D.W. 1998. Evolution of a kyanite bearing pelite belt within a HT-LP orogen: the case of NW Variscan Iberia. *Journal of Metamorphic Geology*, **16,** 379–394.

Schaltegger, U. 1997. Magma pulses in the Central Variscan belt: episodic melt generation and emplacement during lithospheric thinning. *Terra Nova*, **9,** 242–245.

Serrano Pinto, M., Casquet, C., Ibarrola, E., Corretgé, L.G. & Portugal Ferreira, M. 1987. Sintese geocronologica dos granitoides do Maciço Hesperico. *In*: Bea, F., Carnicero, A., Gonzalo, J.C., López Plaza, M. & Rodríguez Alonso, M.B. (eds) *Geología de los granitoides y rocas asociadas del macizo Hespérico*. Universidad de Salamanca, 69–86.

Stacey, J.S. & Kramers, J.D. 1975. Approximation of terrestrial lead isotope evolution by a two stage model. *Earth and Planetary Science Letters*, **26,** 207–221.

Suárez, O., Corretgé, L.G. & Galán, G. 1990. West Asturian-Leonese Zone. Distribution and characteristics of Hercynian metamorphism. *In*: Dallmeyer, R.D. & Martínez García, E. (eds) *Pre-Mesozoic Geology of Iberia*. Springer Verlag, 129–133.

——, Cuesta, A., Corretgé, L.G. & Fernández-Suárez, J. 1992. Spinel-bearing inclusions in calc-alkaline granitoids of the Cantabrian and west Asturian Leonese zones, Hercynian Iberian belt. *Bulletin de la Societé Géologique de France*, **163,** 611–623.

Turner, S., Sandiford, M. & Foden, J. 1992. Some geodynamic and compositional constraints on 'postorogenic' magmatism. *Geology*, **20,** 931–934.

Valverde-Vaquero, P. 1992. *Permo-Carboniferous magmatic activity in the Cantabrian Zone N.E.(Iberian Massif, Asturias, NW Spain)*. MSc Boston College, USA.

——, Cuesta, A., Gallastegui, G., Suárez, O., Corretgé, L.G. & Dunning, G.R. 1999. U-Pb dating of late-Variscan magmatism in the Cantabrian Zone (Northern Spain). *Terra Abstracts*, **11,** 101.

——, Dunning, G.R., Hernaiz-Huerta, P. & Escuder-Viruete, J. 1995. Early-Mid Carboniferous Variscan syn-collisional extension in the Central Iberian Zone (Iberian Massif, Central Spain): Time constraints from the Somosierra area of the Sierra de Guadarrama. *In*: *Abstracts of 26th Annual Meeting of the Tectonic Studies group*.

Vielzeuf, D. & Pin, C. 1989. Geodynamic implications of granulitic rocks in the Hercynian belt. *In*: Daly, J.S., Cliff, R. & Yardley, B.W.D. (eds) *Evolution of Metamorphic Belts*. Geological Society, London, Special Publications, **43,** 343–348.

Villaseca, C., Eugercios, L., Snelling, N., Huertas, M.J. & Castellón, T. 1995. Nuevos datos geocronológicos (Rb-Sr, K-Ar) de granitoides

hercínicos de la Sierra del Guadarrama. *Revista de la Sociedad Geológica de España*, **8,** 137–148.

Yenes, M., Gutiérrez-Alonso, G. & Alvarez, F. 1996. Dtaciones K-Ar de los granitoides del área La Alberca-Béjar (Sistema Central Español). *Geogaceta*, **20,** 479–482.

Zeitler, P.K. & Chamberlain, C.P. 1991. Petrogenetic and tectonic significance of young leucogranites from the northwestern Himalaya, Pakistan. *Tectonics*, **10,** 729–741.

Received 10 May 1999; revised typescript accepted 21 December 1999.
Scientific editing by Randall Parish.